PROCEEDINGS OF SPIE

SPIEDigitalLibrary.org/conference-proceedings-of-spie

Cycling performance of Mn2O3 porous nanocubes and hollow spheres for lithium-ion batteries

Qian Sun
Tik Lun Leung
Kam Chun Sing
Aleksandra B. Djurišić
Mao Hai Xie
Alan M. C. Ng
Hangkong Li
Kaimin Shih

SPIE.

Cycling Performance of Mn_2O_3 Porous Nanocubes and Hollow Spheres for Lithium-ion Batteries

Qian Sun[a], Tik Lun Leung[a], Kam Chun Sing[a], Aleksandra B. Djurišić*[a], Mao Hai. Xie[a], Alan. M. C. Ng[b], Hangkong Li[c], Kaimin Shih[c]
[a]Department of Physics, The University of Hong Kong, Hong Kong, China;
[b]Department of Physics, South University of Science and Technology of China, Shenzhen, China;
[c] Department of Civil Engineering, The University of Hong Kong, Hong Kong, China

ABSTRACT

Mn_2O_3 is a promising anode material for lithium ion battery. Two different kinds of structures of Mn_2O_3 were synthesized via solution processes, the Mn_2O_3 porous cubes and hollow spheres. Scanning electron microscope images and transmission electron microscopy images clearly show the structures. Electrochemical impedance spectroscopy and cyclic voltammetry measurements were used to characterize their electrochemical properties. As anode materials for lithium ion batteries, Mn_2O_3 porous cubes performed similarly as Mn_2O_3 hollow spheres. Both samples started with high initial capacities (1583.2 mAh/g and 1550.7 mAh/g) which were reduced to 173.3 mAh/g and 162.0 mAh/g at 100th cycle at a current density of 100 mA/g. The decrease is likely due to morphology destruction the materials in charging and discharging process.

Keywords: Lithium ion battery, Mn_2O_3, Morphology, Porous structures, Porous cubes, Hollow spheres

1. INTRODUCTION

In recent years, lithium ion batteries (LIBs) are widely used in different areas of electronics in daily life due to their outstanding advantages, for example high energy density, long cycling life and environmentally friendly [1-4]. Researchers are working on improving the energy density and safety of the LIBs as more applications demand higher capacity such as vehicles [5-7]. Nowadays, the most common LIBs in the market are based on graphite anode, whose theoretical capacity is only 372 mAh/g [8-10]. Metal oxides are promising anode materials for they have high capacity and large amount in environment. Transition metal oxides (M_xO_y, M= Co, Ni, Cu, Mn, etc) are most commonly studied. Among the metal oxides, Manganese (III) oxide (Mn_2O_3) is promising due to its theoretical capacity is as high as 1018 mA/g and its abundance in the environment [1]. However, as anode materials for LIBs, Mn_2O_3 has poor cycling stability like other transition metal oxides, due to large volume expansion during charging and discharging process [1, 11]. Hollow and porous structures of Mn_2O_3 were synthesized by researchers to absorb the large volume change during cycling process [12-18]. Su et al. synthesized Mn_2O_3 hollow microspheres via solvent-thermal method. The battery with hollow spheres as anode material could reach a reversible capacity of 580 mAh/g at current density of 500 mA/g after 140 cycles [11]. Huang et al. prepared porous Mn_2O_3 cubes which have initial capacity of 1473 mAh/g and could deliver 845 mAh/g even after 50 cycles [19].

The porous and hollow structures are both effective in buffering the volume changes and therefore keeping the cycling stability of battery. To investigate the effect of hollow structure morphologies, we prepared Mn_2O_3 porous cubes and Mn_2O_3 hollow spheres in same crystal structure in this work and study them as anode materials for LIBs. Solution process is used in both synthesis of the Mn_2O_3 porous cubes and Mn_2O_3 hollow spheres, followed by annealing in the air and the synthesis procedures are simple and efficient. It is found that these two structures of Mn_2O_3 as anode electrodes of LIBs performed similarly for first 100 cycles at a current density of 100 mA/g. Thus, either different synthesis approach or additional volume change buffering strategies are needed to improve the performance.

*dalek@hku.hk; phone +852 2859-7946

Oxide-based Materials and Devices VIII, edited by Ferechteh H. Teherani, David C. Look, David J. Rogers, Ivan Bozovic. Proc. of SPIE Vol. 10105, 1010523 · © 2017 SPIE
CCC code: 0277-786X/17/$18 · doi: 10.1117/12.2251966

2. EXPERIMENTAL DETAILS

2.1 Preparation of Mn_2O_3 porous cubes

In a typical synthesis, 0.474 g of $KMnO_4$ was added into 35 mL ethylene glycol (EG) in a round bottom flask and keeps stirred. After 20 minutes, 1.2 g of NH_4HCO_3 dissolved in 15 mL distilled water was added into the above brown solution and then stirred for another 20 minutes at room temperature. Then the flask was put into an oil bath at 80 ^oC and stirred vigorously for 9 hours and cooled down naturally. The white products were collected after the flask cooled down and washed with deionized water and ethanol three times respectively. Then the solid was dried in vacuum oven at 60 ^oC overnight. Finally, the porous structure was obtained by annealing the powder at 550 ^oC for 8 hours [19].

2.2 Preparation of Mn_2O_3 hollow spheres

Preparation of $MnCO_3$ microspheres. At first, 0.75g (4.44mmol) of $MnSO_4 \cdot H_2O$ and 0.75g of Polyvinylpyrrolidone (PVP) MW10000 was dissolved in 60 mL of deionized water under stirring. After the solution was clear, 30 mL of 0.6 M $NaHCO_3$ was added into the solution and stirred for 1 hour. A white suspension was obtained. The suspension was allowed to settle, and the precipitate was washed with deionized water and ethanol for several times. At last, $MnCO_3$ microsphere was obtained after dried in vacuum oven at 60 ^oC for 12 hours [20].

Preparation of Mn_2O_3 hollow spheres. 0.3 g of $MnCO_3$ microsphere was dispersed in 30 mL of deionized water under stirring. Then 7.5 mL of 0.06 M $KMnO_4$ was added into it and allowed to react for 2 minutes. After that, 15 mL of 2 M HCl was then slowly dropped into the mixture for 2 minutes. The black solid obtained was after being washed with deionized water and dried at 60 °C for 6 hours, followed by heating to 500 °C for 10 hours with ramp rate 10 °C/min [20].

2.3 Materials characterization

As-prepared products were characterized by scanning electron microscope (SEM, Hitachi S-4800), transmission electron microscopy (TEM, Philips CM100) to compare the morphology. X-ray diffraction (XRD) patterns were measured on a Bruker D8 advance diffractometer using Cu Ka radiation (λ= 0.154184 nm) as radiation source.

2.4 Electrochemical measurements

Electrochemical measurements were completed in a coin-cell (CR2032). Working electrode was made by mixing active material (70%), Super-P@Li carbon black (20%), and polyvinylidene fluoride (10%). The mixture was dried in vacuum at 60 ^oC for 12 hours before coating on Cu foil. The coated foil was dried at 120 ^oC in vacuum for 12 h to remove solvent. Then the disk-shaped electrodes with 14 mm diameter were cut and the coin-cells were assembled in a glove box filled with argon. The electrolyte (purchased from MTI Corporation) consisted of 1.0 M $LiPF_6$ in a mixture of ethylene carbonate/dimethyl carbonate/diethyl carbonate (1: 1: 1 in volume). Lithium metal (15.6 mm in diameter, 0.25 mm in thickness) was used as a counter-electrode. The galvanostatic performance was measured by a Land battery test system (LAND-CT2001A) at current density of 100 mA/ g between 3.0 V and 0.01 V. In average, 2.5 to 3.0 mg active material was loaded on Cu foil. The specific capacities were calculated on the basis of the weight of the active material of each electrode. Electrochemical impedance spectroscopy (EIS) and cyclic voltammetry (C-V) measurements were both

carried out using a BioLogic VMP3 electrochemical workstation. EIS measurements were conducted by employing an ac voltage of 5 mV amplitude in the frequency range of 0.01 to 100 kHz, while C-V was measured at the rate of 0.2 mV/s between 0.01 V and 3.0 V.

3. RESULTS AND DISCUSSION

Figure 1 presents X-ray diffraction (XRD) patterns of the Mn_2O_3 porous cubes and Mn_2O_3 hollow spheres. As it is shown in the figure, the major diffraction peaks (211), (222), (400), (332), (431), (440) and (622) are indexed from cubic with Ia-3 space group Mn_2O_3 (JCPDS: 71-0636) in both XRD patterns. The peaks are sharp and intense, which indicate that the samples are highly crystalline. It is clearly seen that there is a small amount of MnO_2 (JCPDS: 72-1982) in Mn_2O_3 porous cubes, while no impurities are found in Mn_2O_3 hollow spheres. The impurity in Mn_2O_3 porous cubes may be caused by incomplete thermal decomposition of $MnCO_3$ in air ($4MnCO_3 + O_2 \rightarrow 2Mn_2O_3 + 4CO_2 \uparrow$) [19].

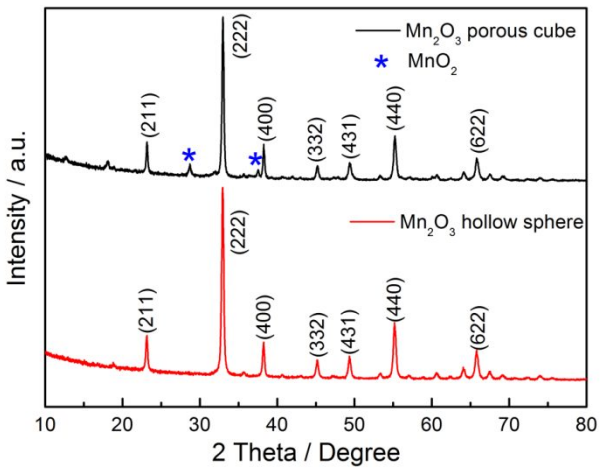

Figure 1. XRD patterns of the Mn_2O_3 porous cubes and Mn_2O_3 hollow spheres. The peaks are labelled according to JCPDS file 71-0636.

The morphologies were characterized by SEM. Figure 2(a) and (b) show the Mn_2O_3 porous cubes after 550 ^oC annealing in different scales. The low-magnification image in figure 2(a) clearly displays the Mn_2O_3 porous cubes. The sizes of uniform cubes were in range of 1.5 - 2 μm. The high-resolution SEM image of figure 2(b) presents the structure more clearly that it is obvious that many pores can be seen in the cubes. However, the Mn_2O_3 hollow spheres were quite different in morphology. As displayed in figure 2(c), the hollow spheres were in different diameters, varied from less than 1.0 μm to more than 2.0 μm. Besides, we can clearly find out that the spheres are hollow inside, since some of the spheres exhibit openings the surface. The surface of the spheres was porous structure as can be seen in figure 2(d). The porous and hollow structures were further characterized by transmission electron microscopy (TEM). As shown in figure 3(a), whole view of a Mn_2O_3 porous cube can be seen with porous structures, and the pores are clearer especially in the edge. In figure 3(b), the darker outside edge and bright inside part in the image obviously indicate the hollow sphere.

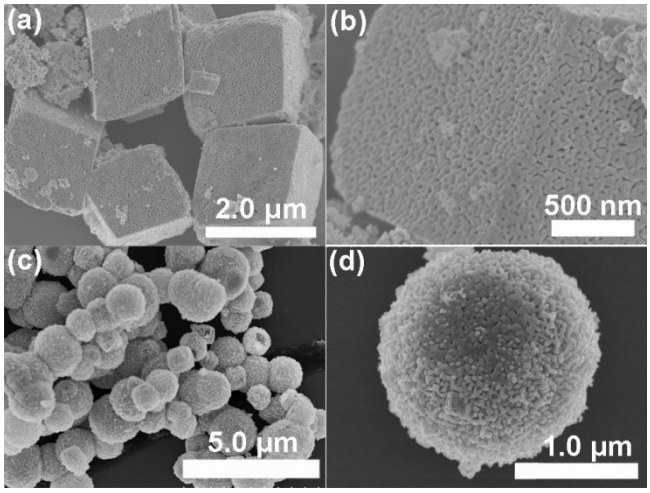

Figure 2. SEM images in different scales of (a) and (b) Mn_2O_3 porous cubes; (c) and (d) Mn_2O_3 hollow spheres.

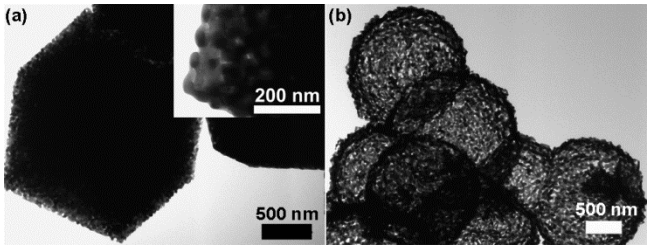

Figure 3. TEM images of (a) the Mn_2O_3 porous cubes and (b) Mn_2O_3 hollow spheres.

The lithium-storage properties and cycling stabilities were measured by the standard half-cell configuration. Figure 4 shows the cycling performance and coulombic efficiency of the two kind's structures of Mn_2O_3. We can clearly tell that both batteries were performed almost the same in cycling and stability. Large initial discharge capacities of 1583.2 mAh/g and 1550.7 mAh/g in the first cycle was obtained of Mn_2O_3 porous cubes and Mn_2O_3 hollow spheres respectively at the current density of 100 mA/g. Then the capacities dropped to 741.0 mAh/g and 709.2 mAh/g separately in the 2^{nd} cycle and both of them decrease slowly afterwards with charging and discharging went on. At about 30^{th} cycles, the capacity of the Mn_2O_3 porous cubes was 244.5 mAh/g and slowly decreased to 173.3 mAh/g at 100^{th} cycles. The same trend was found in Mn_2O_3 hollow spheres, whose capacities were 222.4 mAh/g at 30^{th} cycle and dropped to 162.0 mAh/g at 100^{th} cycles. The Coulombic efficiency of these two kinds of structures is both above 90% from 6^{th} cycle and 98% from 32^{th} cycles. From figure 4, it can be figured out that the capacities dropped quickly from the 1^{st} cycle to the 20^{th} cycle, and the decreasing trend became slow from 20^{th} to 100^{th} cycle with discharging-charging process. The high initial capacity may because of the large theoretical capacity of Mn_2O_3 (1018 mAh/g) and the excess capacities could be generated by the irreversible decomposition of the electrolyte at low voltages. The decrease may be caused by the structure destruction of the Mn_2O_3 and solid electrolyte interphase (SEI) layer formation which is caused by electrolyte decomposition [2, 21]. The Mn_2O_3 is based on conversion (redox) reaction [14] with the counter electrode (Lithium metal) in charging and discharging process. In the conversion reaction process, there are large volume changes after and before the reaction, which easily destroys the nano structure of the material, and results in decrease of capacity. Besides, the SEI layer on the surface of the electrode is a barrier of the diffusion of Li ions in charging and discharging process, which is an important reason for capacity decrease as well [22].

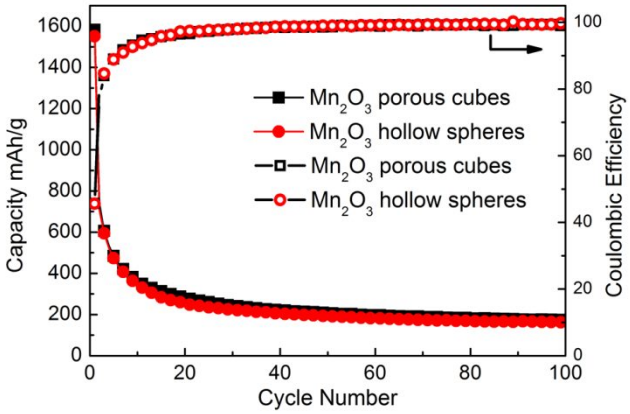

Figure 4. Cycling performance and Coulombic efficiency of the Mn_2O_3 porous cubes and Mn_2O_3 hollow spheres at a current density of 100 mA/g.

Cyclic voltammetry (C-V) and electrochemical impedance spectroscopy (EIS) were applied to further investigate the electrochemical properties. The C-V curves were measured from the half cell at the rate of 0.2 mV/s between 0.01 V and 3.0 V at room temperature. Figure 5(a) shows the C-V curves of the electrode of Mn_2O_3 porous cubes, the first cycle displayed a broad peak at 1.16 V in discharging process, where the reduction of Mn^{3+} to Mn^{2+} may happen, and may be caused by lithium ions insertion. In addition, there is a small and minor peak at 0.622 V, which may be caused by irreversible decomposition of the electrolyte to form a solid electrolyte interface. A small peak appears at 0.14 V, which may be ascribed to the further reduction of Mn^{2+} to Mn^0 [2,4,11,14,19,20,23]. In charging process, an obvious peak appears at 1.26 V, which may be due to the oxidation of Mn^0 to Mn^{2+} [2,4,19,20,23]. After the 1st cycle, there are two reduction peaks and oxidation peaks in the 2nd and 3rd cycles of the two kinds of electrodes, which are corresponded to Mn^{2+} to Mn^0 and Mn^0 to Mn^{2+} [1,19]. The reactions are the same in Figure 5(b) of the C-V curves. In the first cycle, reduction reaction Mn^{3+} to Mn^{2+} may occur at 1.27 V in the discharging part, and at the voltage of 0.86 V, irreversible formation of SEI layer takes place caused by decomposition of the electrolyte. Another peak at 0.04 V is because of the reduction of Mn^{2+} to Mn^0. In the charging process, a wide peak appears at 1.26 V, which may because of the oxidation of Mn^0 to Mn^{2+} [2,4,11,14,19,20,23]. The C-V curves become repeatable after the 1st cycle, and there are two peaks of reduction and oxidation respectively in the 2nd and 3rd cycles of the two kinds of electrodes, which are corresponded to Mn^{2+} to Mn^0 and Mn^0 to Mn^{2+} [23, 24]. The reaction equations are as follows [2, 3, 24, 25]:

$$2Li^+ + 3Mn_2O_3 + 2e^- \rightarrow 2Mn_3O_4 + Li_2O \quad (1)$$

$$2Li^+ + Mn_3O_4 + 2e^- \rightarrow 3MnO + Li_2O \quad (2)$$

$$MnO + 2Li^+ + 2e^- \leftrightarrow 4Li_2O + Mn \quad (3)$$

Impedance studies were conducted of the two structures of Mn_2O_3 by employing an ac voltage of 5 mV amplitude in the frequency range of 0.01 to 100 kHz. Figure 6(a), it shows the impedance changes of initial batteries and after 5 cycles. It is obvious that the R_{ct} of both materials increases with the increase cycle numbers. This may be mainly caused by the SEI formation on the surface of the electrode and the destruction of the materials structure [26].

Figure 7 shows the SEM images of the two structures electrodes after 100 cycles of charging and discharging process. We can clearly tell that the morphologies of the electrodes after 100 cycles are completely different from the original samples. The electrodes were covered with SEI layers on the surface and the porous cubes and hollow spheres structures were destroyed in the process of lithium ions insertion and deinsertion.

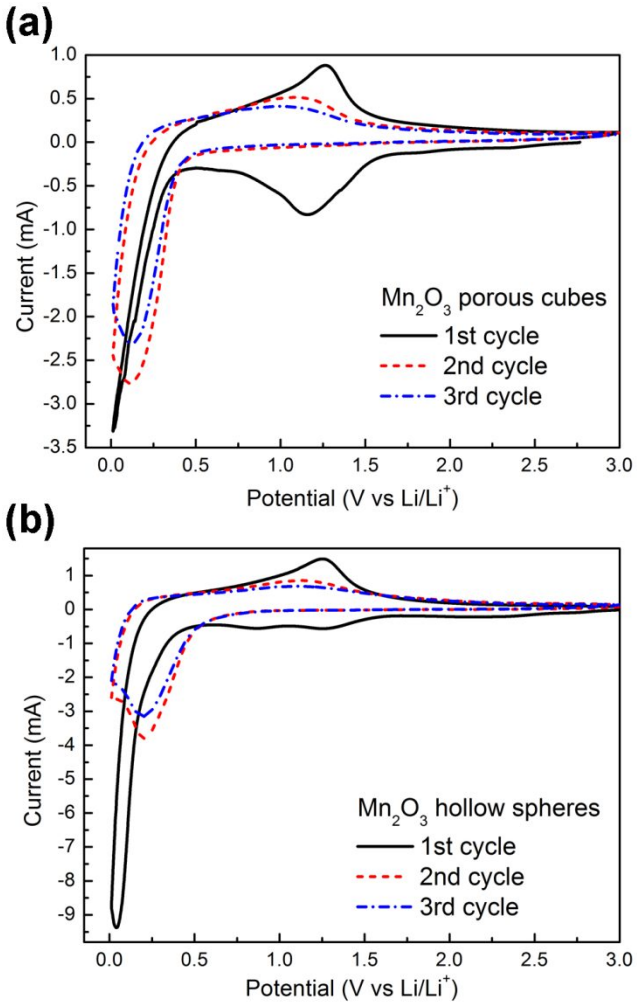

Figure 5. Cyclic voltammetry curves of the batteries, (a) the Mn_2O_3 porous cubes and (b) Mn_2O_3 hollow spheres as the anode materials.

Based on the mechanism of Mn_2O_3 as anode material of lithium ion batteries, the large volume changes in charging and discharging process will completely destroy the nano-structures of the initial materials, which resulting in the quick capacity decrease of the battery. Therefore, buffering the volume expansion is the key point to keep the structures and cycling stability. Carbon shells, ALD coating or graphene sheet wrapping with the porous structure or hollow structure may be effective ways to absorb the volume changes of Mn_2O_3 [27-29] and need further investigation.

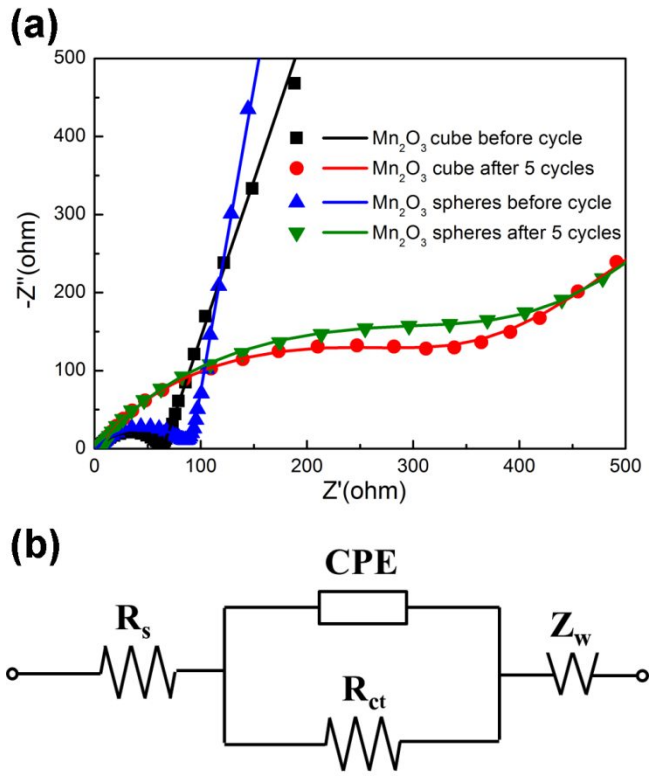

Figure 6. (a) Nyquist plots of the Mn_2O_3 porous cubes and Mn_2O_3 hollow spheres anode materials initial and after 5 cycles, (b) equivalent circuit of the anode materials.

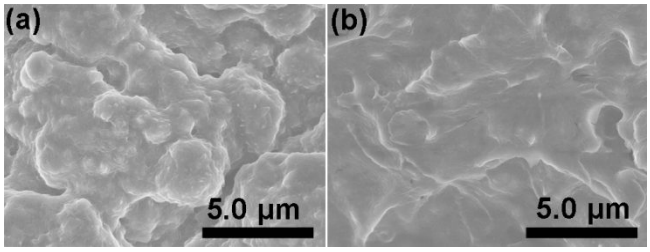

Figure 7. (a) SEM image of the Mn_2O_3 porous cubes and (b) Mn_2O_3 hollow spheres anode electrodes after 100 cycles charging and discharging.

4. CONCLUSIONS

In this work, two kind's structures of Mn_2O_3 were prepared via solution process, the porous cube and hollow spheres. Their morphologies and electrochemical properties were studied. They exhibited similarly as anode materials of lithium ion batteries with high initial capacities and reached 173.3 mAh/g and 162.0 mAh/g at 100 cycles of the porous cubes and hollow spheres electrodes separately. For both samples, impedances become larger as the cycle numbers increase. After 100 cycles of charging and discharging, the porous and hollow structures were both destroyed and covered with EIS layers on the surface. Due to the volume changes during the charging and discharging process, the structure of pure Mn_2O_3 are easily destroyed, and therefore leads to the quick decrease of battery capacity.

Acknowledgement

Financial support from the Strategic Research Theme on Clean Energy and Seed Funding for Applied Research Grant of the University of Hong Kong is acknowledged. The authors would like to thank Prof. K. Y. Chan for the use of the electrochemical workstation.

REFERENCES

[1] Chen, X. Q., Lin, H. B., Zheng, X. W., Cai, X., Xia, P., Zhu, Y. M., Li, X. P. and Li, W. S., "Fabrication of core–shell porous nanocubic Mn_2O_3@TiO_2 as a high-performance anode for lithium ion batteries," J. Mater. Chem. A 3, 18198–18206 (2015).

[2] Hu, L., Sun, Y., Zhang, F. and Chen, Q., "Facile synthesis of porous Mn_2O_3 hierarchical microspheres for lithium battery anode with improved lithium storage properties," J. Alloys Compd. 576, 86-92 (2013).

[3] Yu J., Zhu, L., Fan, C., Zan, C., Hu, L., Yang, S., Zhang, Q., Zhu, W., Shi, L. and Wei, F., "Highly dispersed Mn_2O_3 microspheres- facile solvothermal synthesis and their application as Li-ion battery anodes," Particuology 22, 89-94 (2015).

[4] Han, X., Han, X., Li, R., Sun, L., Lu, K., Wu, M., Zhu, Y. and Zhao, X., "Porous Mn_2O_3 microcubes with exposed {001} facets as electrode for lithium ion batteries," New J. Chem. 40, 6030-6035 (2016).

[5] Bruce, P. G., Scrosati B. and Tarascon J. M., "Nanomaterials for rechargeable lithium batteries," Angew. Chem. Int. Ed. 47, 2930 – 2946 (2008).

[6] Liang, Y., Feng, R., Yang, S., Ma, H., Liang, J. and Chen, J., "Rechargeable Mg batteries with graphene-like MoS_2 cathode and ultrasmall Mg nanoparticle anode," Adv. Mater. 23, 640–643 (2011).

[7] Wang, Y., Li, H., He, P., Hosonoa, E. and Zhou, H., "Nano active materials for lithium-ion batteries," Nanoscale 2, 1294-1305 (2010).

[8] Liu, J., Qian, D., Feng, H., Li, J., Jiang, J., Peng, S. and Liu, Y., "Designed synthesis of TiO_2-modified iron oxides on/among carbon nanotubes as a superior lithium-ion storage material," J. Mater. Chem. A 2, 11372–11381 (2014).

[9] Wang, L., Nie, Z., Cao, C., Zhu, Y. and Khalid, S., "Chrysanthemum-like TiO_2 nanostructures with exceptional reversible capacity and high coulombic efficiency for lithium storage," J. Mater. Chem. A 3, 6402–6407 (2015).

[10] Cheng, J., Wang. B., Xin, H., Kim, C., Nie, F., Li, X., Yang, G. and Huang, H., "Conformal coating of TiO_2 nanorods on a 3-D CNT scaffold by using a CNT film as a nanoreactor: a free-standing and binder-free Li-ion anode," J. Mater. Chem. A 2, 2701–2707 (2014).

[11] Su, H., Xu, Y. F., Feng, S. F., Wu, Z. G., Sun, X. P., Shen, C. H., Wang, J. Q., Li, J. T., Huang, L. and Sun, S. G., "Hierarchical Mn_2O_3 hollow microspheres as anode material of lithium ion battery and its conversion reaction mechanism investigated by XANES," ACS Appl. Mater. Interfaces 7, 8488−8494 (2015).

[12] Chang, L., Mai, L. Xu, X., An, Q., Zhao, Y. and Wang, D., "Pore-controlled synthesis of Mn_2O_3 microspheres for ultralong-life lithium storage electrode," RSC Adv. 3, 1947–1952 (2013).

[13] Qiao, Y., Yu, Y., Jin, Y., Guan, Y. B. and Chen, C. H., "Synthesis and electrochemical properties of porous double-shelled Mn_2O_3 hollow microspheres as a superior anode material for lithium ion batteries," Electrochim. Acta 132, 323–331 (2014).

[14] Lin, H. B., Rong, H. B., Huang, W. Z., Liao, Y. H., Xing, L. D., Xu, M. Q., Li, X. P. and Li, W. S., "Triple-shelled Mn_2O_3 hollow nanocubes: forceinduced synthesis and excellent performance as the anode in lithium-ion batteries," J. Mater. Chem. A 2, 14189–14194 (2014).

[15] Yu, J., Zhu, L., Fan, C., Zan, C., Hu, L., Yang, S., Zhang, Q., Zhu, W., Shi, L. and Wei, F., "Highly dispersed Mn_2O_3 microspheres: Facile solvothermal synthesisand their application as Li-ion battery anodes," Particuology 22, 89–94 (2015).
[16] Dai, Y., Jiang, H., Hu, Y. and Li, C., "Hydrothermal synthesis of hollow Mn_2O_3 nanocones as anode material for Li-ion batteries," RSC Adv. 3, 19778–19781 (2013).
[17] Cai, Y., Liu, S., Yin, X., Hao, Q., Zhang, M. and Wang, T., "Facile preparation of porousone-dimensional Mn_2O_3 nanostructures and their application as anode materials for lithium-ion batteries," Physica E 43, 70–75 (2010).
[18] Wang, Y. Niu, S. and Lu, S., "Controlled synthesis and lithium storage properties of Mn_2O_3 triple-shelled hollow spheres and porous spheres," Mater. Lett. 158, 416–419 (2015).
[19] Huang, S. Z., Jin, J., Cai, Y., Li, Y., Deng, Z., Zeng, J. Y., Liu, J., Wang, C., Hasan, T. and Su, B. L., "Three-Dimensional (3D) Bicontinuous Hierarchically Porous Mn_2O_3 Single Crystals for High Performance Lithium-Ion Batteries," Sci. Rep. 5, 14686 (2015).
[20] Zhang, C. C., Guo, C. L., Wei, Y. H. and Hou, L. F., "A simple synthesis of hollow Mn_2O_3 core–shell microspheres and their application in lithium ion batteries," Phys.Chem.Chem.Phys. 18, 4739 (2016).
[21] Zhou, G., Wang, D. W., Li, F., Zhang, L., Li, N., Wu, Z. S., Wen, L., Lu, G. Q. and Cheng, H. M., "Graphene-wrapped Fe_3O_4 anode material with improved reversible capacity and cyclic stability for lithium ion batteries," Chem. Mater. 22, 5306–5313 (2010).
[22] Reddy, M. V., Subba Rao, G. V. and Chowdari B. V. R., "Metal oxides and oxysalts as anode materials for li ion batteries," Chem. Rev. 113, 5364−5457 (2013).
[23] Zhang, X., Qian, Y., Zhu, Y. and Tang, K., "Synthesis of Mn_2O_3 nanomaterials with controllable porosity and thickness for enhanced lithium-ion batteries performance," Nanoscale 6, 1725–1731 (2014).
[24] Chandra Sekhar, B. and Kalaiselvi N., "Pristine hollow microspheres of Mn_2O_3 as potential anode for lithium-ion batteries," CrystEngComm, 17, 5038-5045 (2015).
[25] Deng, Y., Li, Z., Shi, Z., Xu, H., Peng, F. and Chen, G., "Porous Mn_2O_3 microsphere as a superior anode material for lithium ion batteries," RSC Adv. 2, 4645–4647 (2012).
[26] Chen, S., Liu, F., Xiang. Q., Feng, X. and Qiu, G., "Synthesis of Mn_2O_3 microstructures and their energy storage ability studies," Electrochim. Acta 106, 360– 371 (2013).
[27] Guan, B. Q., Sun, W. W. and Wang, Y., "Carbon-coated $MnMoO_4$ nanorod for high-performance lithium-ion batteries," Electrochim. Acta 190, 354–359 (2016).
[28] Liu, X., Sun, Q., Ng, A. M. C., Djurišić, A. B., Xie, M. H., Dai, B. H., Tang, J., Surya, C., Liao, C. Z. and Shih, K. M., "Alumina stabilized graphene oxide wrapped SnO_2 hollow sphere LIB anode with improved lithium storage," RSC Advances 5, 100783-100789 (2015).
[29] Sun, Q., Liu, X., Djurišić, A. B., Leung, T. L., Xie, M. H., Ng, A. M. C., Li H. K., Deng Z. F. and Shih K. M., "Iron oxide/graphene composites for lithium ion battery anodes-optimum particle size for stable performance," RSC Advances 5, 91466-91471 (2015).